

## High Rate Physics at Neutrino Factories <sup>a</sup>

B.J. King

*Brookhaven National Laboratory, Building 901A, P.O. Box 5000, Upton, NY11973*

*email: bking@bnl.gov*

*web page: <http://pubweb.bnl.gov/people/bking>*

Both muon colliders and non-colliding muon storage rings using muon collider technology have the potential to become the first true “neutrino factories”, with uniquely intense and precisely characterized neutrino beams that could usher in a new era of high rate and long baseline neutrino physics studies at accelerators. This paper gives an overview of the predicted capabilities of neutrino factories for high rate neutrino physics analyses that will use huge event samples collected with novel, high performance neutrino detectors.

### 1 Introduction

The idea of using muon storage rings for neutrino physics is an old one <sup>1</sup>. More recent feasibility studies and design work for muon colliders <sup>2,3</sup> led to investigations <sup>4,5</sup> of the exciting neutrino physics possibilities from the uniquely intense neutrino beams they will produce and, as a variation on this theme that is now attracting very considerable interest, it was then proposed <sup>6</sup> to use muon collider technology for non-colliding muon storage rings dedicated to neutrino physics. An extensive literature <sup>7</sup> is now building up on the impressive potential of both types of “neutrino factories” (or “nufacts”, for short).

Nufacts will be used for each of the two classes of neutrino experiments at accelerators:

1. high rate (HR) experiments, where the detector is placed close to the neutrino source to obtain the most intense beam possible and hence gather very high event statistics of neutrino interactions.
2. long baseline (LB) experiments, where a very massive neutrino detector is placed far away from the neutrino source, deliberately sacrificing event rate in order to study baseline-dependent properties of the neutrinos and, in particular, whether there are “flavor oscillations” in the types of neutrinos composing the beam.

The large muon currents and tight collimation of the neutrinos from nufacts results in extremely intense beams with several important advantages over the neutrino beams produced today from pion decay at accelerator beamlines:

1. event statistics for HR experiments that might be three or more orders-of-magnitude larger than in today’s HR neutrino experiments
2. both higher statistics and longer baselines for LB experiments

---

<sup>a</sup>Presented at the 23rd Johns Hopkins Workshop on Current Problems in Particle Theory, “Neutrinos in the Next Millennium”, Johns Hopkins University, Baltimore MD, June 10-12, 1999.

3. extremely well understood and pure two-component beams with accurately predictable energy spectra, angular divergences and intensities
4. the first high flux electron-neutrino and electron-antineutrino beams at high energies.

Of the two classes of neutrino experiments at nufacts, LB neutrino oscillation studies are currently attracting an enormous amount of interest, with a large and growing literature <sup>7</sup> that includes another paper <sup>8</sup> in these proceedings. This paper will instead concentrate on the less-developed topic of the potential for a rich and broad-based program of HR neutrino physics at nufacts. It summarizes the material covered in a much longer that is in preparation on this topic <sup>9</sup>.

The advantages of neutrino beams from the decays of stored muons over traditional neutrino beams from pion decays are in some ways even more notable for HR experiments than for oscillation studies. In particular, the beam intensity and uniquely small transverse extent close to production invites the use of compact fully-active tracking targets backed by high-rate, high-performance detectors.

In contrast to long baseline neutrino oscillation measurements, the physics interest lies in the interactions of neutrinos rather than in their internal properties. Neutrinos are unique in participating only in the weak interaction and so, for example, they provide a probe of nucleon structure that is intrinsically cleaner than the alternative of charged lepton (electron, positron or muon) scattering. The weak interaction couplings of neutrinos to both quarks and electrons are also interesting in their own right, as will be discussed in the sections 4 and 5 on electroweak measurements and the CKM quark mixing matrix, respectively. Nufacts will also have potential for examining, or searching for, rare and exotic interaction processes. As a bonus outside neutrino physics, HR experiments at nufacts will be impressive factories for the study of charm decays.

The following section presents background material on the expected experimental conditions for HR neutrino physics at nufacts, in preparation for the subsequent physics sections on the topics of nucleon structure and QCD measurements, precision electroweak studies, quark mixing measurements, rare and exotic processes and, last but not least, charm decay physics, before the summary section.

## 2 Experimental Overview

### 2.1 The Neutrino Beam

The beam spectrum from muon decays in a monochromatic muon beam is a completely pure 2-component mixture; the decays of parent  $\mu^-$  provide beams of  $\nu_\mu$  plus  $\bar{\nu}_e$  and  $\mu^+$  decays provide beams of  $\bar{\nu}_\mu$  plus  $\nu_e$ :

$$\begin{aligned}\mu^- &\rightarrow \nu_\mu + \bar{\nu}_e + e^-, \\ \mu^+ &\rightarrow \bar{\nu}_\mu + \nu_e + e^+.\end{aligned}\tag{1}$$

These beams will be denoted as  $(\nu_\mu\bar{\nu}_e)$  and  $(\bar{\nu}_\mu\nu_e)$  in the rest of this paper. The kinematics of a muon decaying to an electron and 2 neutrinos is precisely specified by the electroweak theory and leads to precisely modeled neutrino spectra for HR

physics at nufacts. This is a substantial advantage over conventional neutrino beams from pion decays, particularly for the high-statistics precision measurements that will be described in sections 3 through 5.

Reference <sup>9</sup> derives explicit expressions for the beam spectra at high rate experiments in the context of a simplified but relatively realistic model of a thin, monochromatic muon beam in the production straight section of the storage ring. The derivations assume zero net polarization over the data sample; in order to minimize beam modeling systematics in experimental analyses, it is likely that the storage ring will be designed so that the muon polarization precesses to average to zero over each fill of muons.

The derivation in reference <sup>9</sup> begins from the neutrino energy distributions in the rest frame of the decaying muon,  $E'_\nu$ , where the scaled energy,  $x \equiv 2E'_\nu/m_\mu$ , has a distribution given by

$$\begin{aligned}\frac{dN_{\nu_\mu}}{dx} &= 6.x^2 - 4.x^3 \\ \frac{dN_{\nu_e}}{dx} &= 12.x^2 - 12.x^3\end{aligned}\tag{2}$$

for muon-type neutrinos or anti-neutrinos and for electron-type neutrinos or anti-neutrinos, respectively. It is shown that  $x$  is simply related to the neutrino energy in the laboratory frame,  $E_\nu$ , by:

$$E_\nu(x, \theta') = x \frac{E_\mu}{2} (1 + \beta \cos \theta'),\tag{3}$$

where  $\beta = 1$  to a very good approximation and each angle in the muon rest frame,  $\theta'$  corresponds to an angle  $\theta$  in the laboratory frame according to:

$$\sin \theta = \frac{\sin \theta'}{\gamma(1 + \beta \cos \theta')},\tag{4}$$

where  $\gamma \equiv \frac{E_\mu}{m_\mu c^2}$ . Equation 3 combined with equations 2 and 4 therefore specifies the neutrino energy spectra at any position in an experimental target, at least in this simplified model.

Substituting the specific value  $\theta' = \frac{\pi}{2}$  into equation 4 shows that the forward hemisphere in the muon rest frame is boosted into a narrow cone of half angle

$$\theta_\nu \simeq \sin \theta_\nu = 1/\gamma = \frac{m_\mu c^2}{E_\mu} \simeq \frac{0.106}{E_\mu[\text{GeV}]}.\tag{5}$$

This characteristic opening half-angle with respect to the muon beam direction will include approximately half of the neutrinos in the thin pencil beams for HR experiments at nufacts and the radius subtended by this angle at the experimental target is a reasonable choice for the radius of the target. This corresponds, for example to a 20 cm radius at 100 m from production in a 50 GeV muon beam or at 1 km from a 500 GeV muon beam.

## 2.2 Primer on Neutrino-Nucleon Deep Inelastic Scattering

The dominant weak interaction processes for many-GeV neutrinos and anti-neutrinos are charged current (CC) and neutral current (NC) deep inelastic scattering (DIS) off nucleons (N, i.e. protons and neutrons) with the production of several hadrons ( $X$ ):

$$\begin{aligned}
 \nu(\bar{\nu}) + N &\rightarrow \nu(\bar{\nu}) + X && (NC) \\
 \nu + N &\rightarrow l^- + X && (\nu - CC) \\
 \bar{\nu} + N &\rightarrow l^+ + X && (\bar{\nu} - CC),
 \end{aligned} \tag{6}$$

where the charged lepton,  $l$ , is an electron/muon for electron/muon neutrinos. The interaction of neutrinos with electrons is three orders of magnitude less common than neutrino-nucleon DIS. From the property of lepton universality, the DIS interactions  $\nu_e$ 's and  $\nu_\mu$ 's, or of their anti-neutrinos, are expected to be identical up to final-state lepton mass corrections that are calculable and almost negligible for multi-GeV neutrinos. This simplifies the physics analyses and allows for a useful check of experimental systematics through the comparison of DIS event samples from the two neutrino flavors. The CC (NC) DIS interactions are well described by the ‘‘naive quark-parton model’’ as quasi-elastic (elastic) scattering off one of the many quarks ( $q$ ) inside the nucleon through the exchange of a virtual W (Z) boson:

$$\nu(\bar{\nu}) + q \rightarrow \nu(\bar{\nu}) + q \quad (NC) \tag{7}$$

$$\nu + q^{(-)} \rightarrow l^- + q^{(+)} \quad (\nu - CC) \tag{8}$$

$$\bar{\nu} + q^{(+)} \rightarrow l^+ + q^{(-)} \quad (\bar{\nu} - CC), \tag{9}$$

To conserve charge, the initial-state and final-state quarks in equations 8 and 9 differ by one unit of charge and have been labelled accordingly, where  $q^{(-)} \in d, s, \bar{u}, \bar{c}$  and  $q^{(+)} \in u, c, \bar{d}, \bar{s}$ . The final state quark always ‘‘hadronizes’’ at the nuclear distance scale, producing quark-antiquark pairs that arrange into the several hadrons seen in the detector.

The naive quark-parton model will be used in the rest of this paper to give qualitative understanding of physics processes, although it should be understood that the actual analyses will require more sophisticated modeling.

## 2.3 The Role of High Performance Neutrino Detectors

The huge reduction in the neutrino beam cross section over the conventional meters-wide beams from pion decay allows the use, for the first time in neutrino physics, of compact, specialized targets surrounded by high performance detectors. As an example, figure 1 illustrates the sort of HR general purpose neutrino detector that would be well matched to the intense neutrino beams at nufacts. (Subsection 3.2, on polarized targets, and subsection 4.1, on neutrino-electron scattering will discuss other possible examples of specialized targets and detectors.)

The neutrino target in figure 1 forms a notable contrast with the kiloton-scale calorimetric targets used in today’s HR neutrino experiments. Instead, it might comprise a 2 meter long stack of CCD tracking planes with a radius of 20 cm chosen

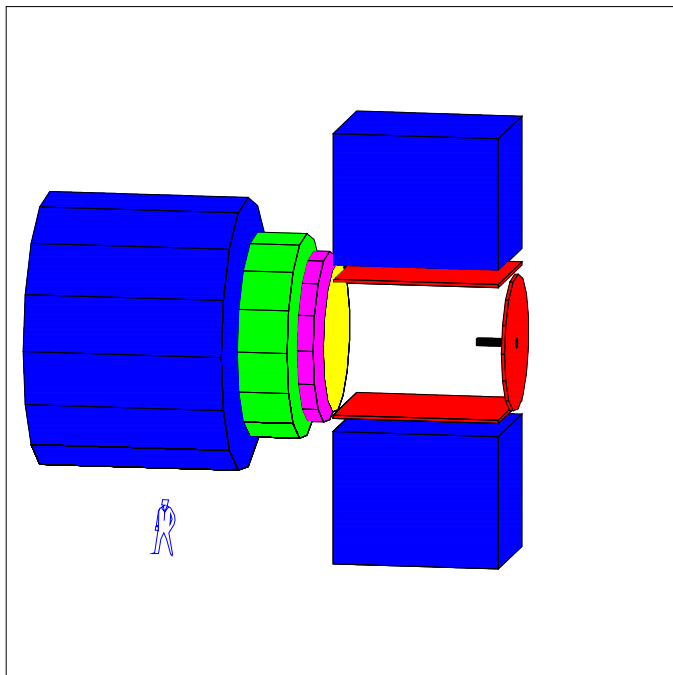


Figure 1: Example of a general purpose neutrino detector. A human figure in the lower left corner illustrates its size. The neutrino target is the small horizontal cylinder at mid-height on the right hand side of the detector. Its radial extent corresponds roughly to the radial spread of the neutrino pencil beam, which is incident from the right hand side. Further details are given in the text.

to match the beam radius at approximately 100 meters from production for a 50 GeV muon beam. As a detailed example, it might contain 1500 planes of 300 micron thick silicon CCD's, corresponding to a mass per unit area of approximately  $100 \text{ g.cm}^{-2}$ , about 5 radiation lengths and one interaction length. (Further parameters for this target will be presented in the following subsection.)

Besides providing the mass for neutrino interactions, a tracking target will allow precise reconstruction of the event topologies from charged tracks, including event-by-event vertex tagging of those events containing charm hadrons or tau leptons and, with the higher energy beams, beauty hadrons. Given the favorable vertexing geometry and the  $\sim 3.5 \mu\text{m}$  typical <sup>10</sup> CCD hit resolutions, it is reasonable to expect <sup>9</sup> perhaps 50 percent efficiency for charm tagging and ultrapure tagging for the relatively rare beauty hadrons that will appear at the higher energies.

The target in figure 1 is surrounded by a projection chamber (TPC) tracker in a vertical dipole magnetic field. The characteristic  $dE/dx$  signatures from the tracks would identify each charged particle. Further particle ID is provided by the Cherenkov photons that are produced in the TPC gas then reflected by a spherical mirror at the downstream end of the tracker and focused onto a read-out plane at the upstream end of the target. The mirror is backed by electromagnetic and hadronic calorimeters and, lastly, by iron-core toroidal magnets for muon ID.

The relativistically invariant quantities that are routinely extracted in DIS experiments, along with their interpretations in the naive quark-parton model, are 1) Feynman  $x$ , the fraction of the nucleon 4-momentum carried by the struck quark, 2) the inelasticity,  $y = E_{\text{hadronic}}/E_\nu$ , which is related to the scattering angle of the neutrino in the neutrino-quark CoM frame (where  $E_{\text{hadronic}}$  is the energy contained in the hadron shower), and 3) the momentum-transfer-squared,  $Q^2 = 2M_p E_\nu xy$  for  $M_p$  the mass of the proton. The high performance detectors at nufacts will have the further capability of reconstructing the hadronic 4-vector, resulting in a much better characterization of each interaction, particularly for NC interactions.

#### 2.4 Cross Sections and Event Rates

This section derives approximate estimates of the event sample sizes expected in HR targets at nufacts.

The DIS cross sections for multi-GeV neutrinos are approximately proportional to the neutrino energy,  $E_\nu$ , and the charged current (CC) and neutral current (NC) interaction cross sections for neutrinos and antineutrinos have numerical values of <sup>11</sup>:

$$\sigma_{\nu N} \text{ for } \begin{pmatrix} \nu - CC \\ \nu - NC \\ \bar{\nu} - CC \\ \bar{\nu} - NC \end{pmatrix} \simeq \begin{pmatrix} 0.72 \\ 0.23 \\ 0.38 \\ 0.13 \end{pmatrix} \times E_\nu [\text{GeV}] \times 10^{-38} \text{ cm}^2. \quad (10)$$

This energy dependence allows us to express the number of DIS events in a target as the simple product of the average beam energy,  $\langle E_\nu \rangle$ , and the integrated luminosity:

$$\text{No. DIS events} = \sigma_{\nu N}^R [\text{cm}^2 \cdot \text{GeV}^{-1}] \times \langle E_\nu \rangle [\text{GeV}] \times \int L dt [\text{cm}^{-2}] \quad (11)$$

where the units are given in square brackets and the constant of proportionality is the reduced cross section defined by:

$$\sigma_{\nu N}^R \equiv \sigma_{\nu N} / E_\nu. \quad (12)$$

Summing equation 10 over NC and CC interactions and averaging over neutrinos and anti-neutrinos gives the numerical value of

$$\sigma_{\nu N}^R = 0.73 \times 10^{-38} \text{ cm}^2 \cdot \text{GeV}^{-1}. \quad (13)$$

For a target subtending  $\theta_\nu = 1/\gamma$  from the production straight section, the number of neutrinos passing through the target is seen to be exactly equal to the number of muon decays,  $N_\mu^{ss}$ , since each muon decay produces two neutrinos but only half of them will be in the forward hemisphere in the muon rest frame. In this case, the total integrated luminosity into the detector is clearly

$$\int L dt [\text{cm}^{-2}] = 6.022 \times 10^{23} \times N_\mu^{ss} \times l [\text{g} \cdot \text{cm}^{-2}], \quad (14)$$

where  $6.022 \times 10^{23}$  is Avogadro's number and  $l [\text{g} \cdot \text{cm}^{-2}]$  is the detector mass per unit area in appropriate units.

Table 1: Specifications, integrated luminosities and event rates for the HR targets discussed in this paper and for 50 GeV (500 GeV) muon storage rings. The approximation is made that the target is situated 100 m (1 km) downstream from a straight section that has  $N_\mu^{ss} = 10^{20}$  decays of 50 GeV (500 GeV) muons. This corresponds to average neutrino energies of 32.5 GeV (325 GeV) and to approximately 1 (2) years running for storage ring parameters given previously in the literature.

target purpose	general	polarized	$\nu - e$ scatt.
material	Si CCD's	solid HD	liquid CH <sub>4</sub>
ave. density	0.5 g.cm <sup>-3</sup>	0.267 g.cm <sup>-3</sup>	0.717 g.cm <sup>-3</sup>
length	2 m	0.5 m	20 m
mass/area, $l$	100 g.cm <sup>-2</sup>	13.4 g.cm <sup>-2</sup>	1434 g.cm <sup>-2</sup>
radius	0.2 m	0.2 m	0.2 m
mass	126 kg	16.8 kg	1800 kg
$\int Ldt$	$6.0 \times 10^{45}$ cm <sup>-2</sup>	$8.1 \times 10^{44}$ cm <sup>-2</sup>	$8.6 \times 10^{46}$ cm <sup>-2</sup>
no. DIS events:			
at 50 GeV	$1.4 \times 10^9$	$1.9 \times 10^8$	$2.0 \times 10^{10}$
at 500 GeV	$1.4 \times 10^{10}$	$1.9 \times 10^9$	$2.0 \times 10^{11}$
no. $\nu$ -e events:			
at 50 GeV	$3.5 \times 10^5$	NA	$7 \times 10^6$
at 500 GeV	$3.5 \times 10^6$	NA	$7 \times 10^7$

Table 1 gives a summary of some characteristics for examples of the three types of targets discussed in this paper, and also gives realistic but very approximate integrated luminosities and event sample sizes for 2 illustrative nufact energies: 50 GeV and 500 GeV. A muon beam energy of about 50 GeV is a likely choice for a dedicated muon storage ring<sup>12</sup>, with default specifications of  $10^{20}$  muon decays per year in the straight section providing the neutrino beams. Five hundred GeV muons corresponds to a 1 TeV center-of-mass muon collider and this parameter set is discussed in reference<sup>9</sup>.

The event samples in table 1 are truly impressive. It is seen, for example, that high performance detectors with fully-active tracking neutrino targets might collect and precisely reconstruct data samples with many billions of neutrino-nucleon DIS interactions – more than three orders of magnitude larger than any of the data samples collected using today's much larger and cruder neutrino targets.

### 3 Nucleon Structure Functions and QCD Studies

#### 3.1 Structure Function Measurements with Unpolarized Targets

It can be shown quite generally that the differential cross sections for neutrino-nucleon and anti-neutrino interactions can be written in terms of nucleon *structure functions* (SF),  $F_1$ ,  $F_2$  and  $F_3$ , as:

$$\frac{d^2\sigma^{\nu(\bar{\nu})}}{dxdy} = \frac{G_F^2 M_p E_\nu}{\pi} \left[ xy^2 F_1^{\nu(\bar{\nu})} + (1-y) F_2^{\nu(\bar{\nu})} \mp xy(1-y/2) F_3^{\nu(\bar{\nu})} \right], \quad (15)$$

with  $G_F$  the Fermi coupling constant,  $M_p$  the proton mass and  $x$  and  $y$  in 2.3 and where small correction factors have been neglected for simplicity. The SF are found to exhibit approximate scaling behavior for  $Q^2 \rightarrow \infty$ , i.e.  $F_i(x, Q^2) \rightarrow F_i(x)$ , which is an encouraging approximate verification of the exact scaling behaviour that is predicted in the naive quark-parton model.

The SF must be experimentally determined by measuring the differential cross sections as functions of  $x$ ,  $y$  and  $Q^2$  and extracting the SF using binned fits that exploit their differing  $y$  dependences. The parity-violating structure function,  $xF_3$ , can only be measured in neutrino-nucleon scattering (and at HERA, although much less precisely and in a different kinematic regime). The  $F_1$  and  $F_2$  SF's that are defined for neutrino-nucleon scattering also probe different combinations of quarks to the analagous SF's defined for charged lepton DIS experiments.

Superscripts on the SF in equation 15 distinguish the potentially different structure functions for  $\nu$  and  $\bar{\nu}$  scattering. However, neutrino experiments to date on isoscalar targets have struggled to resolve the differences, due to insufficient statistics and insufficient control of experimental systematics. Nufacts will therefore provide the first clean extractions of all 6 SF's and this will provide an opportunity that is unique, for any physics process, to lay bare the quark-by-quark content of the nucleon. This will now be made plausible using a simplified discussion in the context of the naive quark-parton model.

In the framework of the naive quark-parton model, the SF can be expressed in terms of quark densities as:

$$\begin{aligned}
2F_1^{\nu N}(x, Q^2) &= d(x) + s(x) + \bar{u}(x) + \bar{c}(x) \\
2F_1^{\bar{\nu} N}(x, Q^2) &= u(x) + c(x) + \bar{d}(x) + \bar{s}(x) \\
F_3^{\nu N}(x, Q^2) &= d(x) + s(x) - \bar{u}(x) - \bar{c}(x) \\
F_3^{\bar{\nu} N}(x, Q^2) &= u(x) + c(x) - \bar{d}(x) - \bar{s}(x)
\end{aligned}
\tag{16}$$

and

$$F_2(x, Q^2) \equiv 2xF_1(x, Q^2).\tag{17}$$

An isoscalar target (i.e. equal numbers of neutrons and protons, as is the case for the silicon tracking target of subsection 2.3) is expected to provide four further approximate equalities:

$$\begin{aligned}
u(x) &= d(x) \\
\bar{u}(x) &= \bar{d}(x) \\
s(x) &= \bar{s}(x) \\
c(x) &= \bar{c}(x).
\end{aligned}
\tag{18}$$

The 8 equations in 16 and 18 can therefore be solved in this naive model to derive, from the measured SF's, the quark-by-quark density distributions, at each  $x$ , for isoscalar targets. (In detail, the first two equations of 16 are actually identical in this simplified model, so additional information from, e.g., charm tagging is needed to completely solve for all of the quark densities.)



As an extension of this argument, SF measurements from both hydrogen and deuterium targets would, using isospin symmetry, give measurements of the quark-by-quark densities in both protons and neutrons. Thus, even the polarization-averaged measurements from the polarized hydrogen targets in subsection 3.2 will clearly be extremely valuable.

In real life, there will clearly be complications beyond the simple picture from the naive quark model, including nuclear effects, so-called “higher twist” processes and charm thresholds, to name just a few. Despite the complications, the above discussion amounts to at least a plausibility argument that nufacts will, for the first time in any experimental process, have the potential to disentangle the quark-by-quark structure of isoscalar nuclear targets, protons and neutrons.

The uniquely precise and detailed quark-by-quark characterization of nucleon structure will provide an invaluable reference source for many diverse analyses in collider and fixed target physics including, of course, the other precision analyses at nufacts. Precise measurements at high  $x$ ,  $x \rightarrow 1$ , are particularly relevant to the modeling of rates for interesting physics processes and backgrounds at hadron colliders.

The universality and applicability of the quark-parton model will be able to be further tested by comparing the nufact SF’s with those from charged lepton DIS measurements, where the quarks couple to the electromagnetic current in proportion to their charge squared. As an example, the quark model relationship between the  $F_2$  structure functions is

$$F_2^u = \frac{5}{18}F_2^\nu + \frac{1}{6}x(s(x) + \bar{s}(x)). \quad (19)$$

Current global SF analyses find puzzling deviations from this relationship at low  $x$  which, it is speculated, might be related to differing nuclear shadowing effects and would vanish for simple nucleon targets. A first high-statistics measurement of  $F_2^\nu$  on deuterium at a nufact that can be compared with existing  $F_2^u$  measurements on deuterium might well resolve the discrepancy.

As the second broad area for SF studies at nufacts, DIS has long been a dominant process in testing and understanding perturbative quantum chromodynamics (pQCD). For example, the scaling behavior of the  $xF_3$  SF is broken by a predictable pQCD evolution that is logarithmic in  $Q^2$  and is independent, to first order in perturbation theory, of the nucleon’s gluon distribution. The observed evolution of  $xF_3$  in  $\nu N$  scattering already provides one of the most precise measurements of the strong coupling constant,  $\alpha_s$ , as does its integral over  $x$ :

$$\int_0^1 F_3(x, Q^2)dx = 3 \left[ 1 - \frac{\alpha_s}{\pi} + O\left(\frac{\alpha_s}{\pi}\right)^2 \right], \quad (20)$$

a measurement known as the Gross Llewellyn-Smith (GLS) Sum Rule. Both of these measurements of  $\alpha_s$  are currently limited by experimental systematic uncertainties and great improvements can be expected with the superior experimental conditions at nufacts.

Heavy quark production in neutrino interactions will provide both additional complications and opportunities for pQCD studies, due to the additional mass

scale,  $m_Q$ , for  $Q = c, b$ . Nufacts will provide a unique facility to test and extend theoretical treatments on this topic. Improved understanding will be valuable for pQCD analyses both within and beyond neutrino physics and, for example, correct modeling of the heavy quark threshold suppression is vital for the CKM studies of section 5.

In addition to these inclusive charm production studies, semi-inclusive measurements involving, for example, the production of  $\Lambda_C^\pm$  or  $J/\psi$ 's will provide opportunities for further insights into QCD, as is addressed elsewhere in these proceedings <sup>13</sup>.

### 3.2 Measurements with Polarized Targets

As well as vastly improving on today's  $\nu N$  SF measurements with unpolarized targets, nufacts will provide the first neutrino beams with sufficient intensity to allow the use of polarized targets. Neutrino scattering experiments using polarized targets have considerable potential for further resolution of the structure of the nucleon and for additional tests of QCD, even at the lower energy beams of dedicated nufacts.

Polarized lepton-nucleon DIS studies have so far been the domain of charged lepton experiments, where a rich program includes SLAC E155x, the recently approved COMPASS experiment at CERN, HERMES at DESY, ELSA in Bonn, MAMI in Mainz and experiments at the Thomas Jefferson National Accelerator Facility. Related studies at collider energies will soon become available in polarized proton-proton collisions at BNL's RHIC collider, and HERA may also eventually polarize their protons beam to provide polarized positron-proton collisions at center-of-momentum energies of approximately 300 GeV.

Polarized neutrino-nucleon scattering retains the experimental advantages over charged lepton DIS experiments that were discussed in subsection 3.1 for non-polarized targets. In addition, the absence of significant target heating from the beam will allow the use of polarized solid protium-deuterium (HD) targets that cannot survive in charged lepton experiments and have so far only been used in experiments with low intensity neutron or photon <sup>14</sup> beams. The preparation of such targets is a detailed craft <sup>15</sup> involving doping the targets with ortho-hydrogen and holding them for long periods of time at very low temperatures and high magnetic fields, e.g. 30-40 days at 17 T and 15 mK. In order to avoid building an entire new detector around the polarized target, it would be economical to place the polarized target directly upstream from another detector, such as the tracking detector described in subsection 2.3.

The polarized SF that might be measured at a nufact are the transversely-polarized and longitudinally-polarized parity-conserving spin-SF's,  $g_1$  and  $g_2$ , respectively, as well as the parity-violating spin-SF  $g_5$ .

As was discussed above for the unpolarized parity-violating SF,  $xF_3$ , polarized target experiments at nufacts should provide easily the most precise measurements of the parity-violating spin structure functions,  $g_5$ , that can only be measured in CC weak interactions. The only other future opportunity to measure  $g_5$  that has been widely discussed is the possibility of eventually polarizing the proton beams in the HERA e-p collider. Because of kinematic constraints on reconstructing events, a polarized HERA would be able to make less precise measurements <sup>16</sup> for protons

in the complementary high  $Q^2$  region,  $Q^2 > 225 \text{ GeV}^2$ , that will not be accessible to nufacts. It would not provide measurements for neutrons, of course.

The quark content for the polarized SF's in the naive quark model is as follows:

$$\begin{aligned}
g_1^{\nu N} &= \Delta d + \Delta s + \Delta \bar{u} + \Delta \bar{c} \\
g_1^{\bar{\nu} N} &= \Delta u + \Delta c + \Delta \bar{d} + \Delta \bar{s}, \\
g_2^{\nu N} &= 0 \\
g_2^{\bar{\nu} N} &= 0 \\
g_5^{\nu N} &= \Delta d + \Delta s - \Delta \bar{u} - \Delta \bar{c} \\
g_5^{\bar{\nu} N} &= \Delta u + \Delta c - \Delta \bar{d} - \Delta \bar{s},
\end{aligned} \tag{21}$$

where each  $\Delta q \equiv q^{\uparrow\uparrow} - q^{\uparrow\downarrow}$  is the difference between quarks polarized parallel to the nucleon spin and those polarized anti-parallel. By similar arguments to that presented in subsection 3.1 for unpolarized SF's it can be seen that the measurement of the polarized SF's for both protons and neutrons should provide much information about the quark-by-quark spin content of the nucleon. This should give nufacts a central role in resolving the current so-called ‘‘spin crisis’’ that has been a dominant topic for DIS spin experiments over the last decade, as follows.

The spin crisis refers to the experimental observation<sup>17</sup> that only a small fraction of the nucleon spin is contributed by the quarks, which was considered to be counter-intuitive and has led to efforts to investigate the other possible contributions to the spin. The contributions are summarized in the helicity sum rule for the nucleon's longitudinal spin,  $S_z^N$ :

$$S_z^N = \frac{1}{2} = \frac{1}{2}(\Delta u + \Delta d + \Delta s) + L_q + \Delta G + L_G, \tag{22}$$

where the quark contribution is  $\Delta\Sigma = \Delta u + \Delta d + \Delta s$ ,  $\Delta G$  is the gluon spin and  $L_q$  and  $L_G$  are the possible angular momentum contributions from the quarks and gluons circulating in the nucleon.

The above method for extracting the various quark spin distributions at nufacts, from inclusive SF, should be much cleaner theoretically than the semi-inclusive measurements needed in charged lepton experiments, which rely on semi-inclusive measurements plus assumptions about fragmentation functions. Even so, nufacts should also provide novel and extended capabilities for such semi-inclusive measurements. They can use, for example, the semi-muonic tagging of charm production. This can be calibrated by vertex-tagging experiments in other detectors and is sensitive to the spin of the strange quarks in the nucleon and, perhaps in some kinematic regions, to the spin contribution of the gluon. Such a capability, if realized, would be very valuable in solving the spin crisis, particularly since the gluon contribution is extremely hard to measure and yet it is the leading suspect for providing the bulk of the nucleon's spin.

#### 4 Precision Electroweak Studies

Nufacts will improve enormously on current neutrino experiments in allowing access to aspects of the electroweak interaction that cannot be readily probed at colliders.

As the most important single electroweak topic, they might well restore the historical role of neutrino scattering experiments in providing some of the most precise measurements of the weak mixing angle,  $\sin^2 \theta_W$ . The electroweak theory predicts that  $\sin^2 \theta_W$  is related to the mass ratio of the W and Z intermediate vector bosons:

$$\sin^2 \theta_W = 1 - \left( \frac{M_W}{M_Z} \right)^2 \quad (23)$$

to first order in perturbation theory. Precise measurements in various processes can probe higher order diagrams to test the consistency of the electroweak theory and provide differing sensitivities to new physics processes occurring, for example, through loop diagram contributions to the scattering amplitudes.

Nufacts should provide vastly improved determinations of the weak mixing angle,  $\sin^2 \theta_W$ , in measurements from (i) the ratio of neutral current (NC) to charged current (CC) DIS events and (ii) measuring absolute cross sections for neutrino-electron scattering, as discussed in the following subsections.

#### 4.1 Neutrino-Electron Scattering

Neutrino-electron elastic scattering,

$$\nu e^- \rightarrow \nu e^-, \quad (24)$$

is an interaction between point elementary particles with a precise theoretical prediction for its cross section as a function of  $\sin^2 \theta_W$ . It therefore provides measurements of  $\sin^2 \theta_W$  that will be essentially limited only by statistics (3 orders of magnitude down from DIS) and by ingenuity in minimizing the experimental uncertainties.

Four different  $\nu$ -e elastic scattering processes occur in total in the  $(\nu_\mu \bar{\nu}_e)$  and  $(\bar{\nu}_\mu \nu_e)$  beams:

$$\nu_\mu e^- \rightarrow \nu_\mu e^- \quad (25)$$

$$\bar{\nu}_e e^- \rightarrow \bar{\nu}_e e^- \quad (26)$$

$$\bar{\nu}_\mu e^- \rightarrow \bar{\nu}_\mu e^- \quad (27)$$

$$\nu_e e^- \rightarrow \nu_e e^-, \quad (28)$$

where the first two processes occur in the  $(\nu_\mu \bar{\nu}_e)$  beam and the final two in the  $(\bar{\nu}_\mu \nu_e)$  beam. The two scattering processes in a given beam cannot be experimentally separated so the experimental measurement involves counting the sum of events from the two processes. The  $(\nu_\mu \bar{\nu}_e)$  and  $(\bar{\nu}_\mu \nu_e)$  beams will provide two physically distinct measurements because the scattering involves different diagrams for the neutrino species in the two beams: an s-channel (annihilation) diagram contributes to equation 26 while equation 28 includes a charged current ( $W^\pm$  exchange) t-channel diagram.

Because of the small ratio of the electron to proton mass, the cross section for neutrino-electron scattering is much smaller than that for DIS. The numerical

Reaction	$g_L$	$g_R$	$g_L^2 + \frac{1}{3}g_R^2$
$\nu_\mu e^- \rightarrow \nu_\mu e^-$	$-\frac{1}{2} + \sin^2 \theta_W$	$\sin^2 \theta_W$	0.0925
$\bar{\nu}_e e^- \rightarrow \bar{\nu}_e e^-$	$\sin^2 \theta_W$	$\frac{1}{2} + \sin^2 \theta_W$	0.2258
$\bar{\nu}_\mu e^- \rightarrow \bar{\nu}_\mu e^-$	$\sin^2 \theta_W$	$-\frac{1}{2} + \sin^2 \theta_W$	0.0758
$\nu_e e^- \rightarrow \nu_e e^-$	$\frac{1}{2} + \sin^2 \theta_W$	$\sin^2 \theta_W$	0.5425

Table 2:  $g_L$  and  $g_R$  by  $\nu - e$  scattering process listed for the cross section formula in equation 29. The value  $\sin^2 \theta_W = 0.225$  has been used for the final column.

values for the cross sections after integrating over  $y$  are:

$$\sigma(\nu e^- \rightarrow \nu e^-) = 1.6 \times 10^{-41} \times E_\nu [GeV] \times \left[ g_L^2 + \frac{1}{3} g_R^2 \right], \quad (29)$$

where the left-handed and right-handed coupling constants,  $g_L$  and  $g_R$ , are different for each of the processes in equations 27 through 26. Their values and the values for the term in square brackets are given in table 4.1.

The experimental signature for  $\nu - e$  scattering is a single negatively charged electron with very low transverse momentum,  $p_t \lesssim \sqrt{m_e E_\nu}$ . A tracking detector with very good  $p_t$  resolution is needed to resolve the signal peak from the much broader background distributions from quasi-elastic  $\nu - N$  scattering and other low-multiplicity  $\nu - N$  scattering events. An attractive target/detector option is a low-Z liquid that can form tracks of ionization electrons and drift them to an electronic read-out. Liquids under consideration<sup>9</sup> include argon and methane or other saturated alkanes, and the readout geometry might be a TPC or, to reduce pile-up backgrounds, a printed-circuit kaptan strip geometry<sup>18</sup> with more channels and shorter drift distances.

Besides background rejection, the other big experimental challenge for the measurement will be the determination of the absolute neutrino flux. For the  $(\nu_\mu \bar{\nu}_e)$  beam, signal processes can probably<sup>9</sup> be precisely normalized to the theoretically predictable processes involving muon production off electrons:  $\nu_\mu e^- \rightarrow \nu_\mu \mu^-$  and  $\bar{\nu}_e e^- \rightarrow \bar{\nu}_e \mu^-$ . The  $(\bar{\nu}_\mu \nu_e)$  beam requires an additional stage of relative flux normalization, which might be accomplished<sup>9</sup> using the relative sizes of the event samples for quasi-elastic neutrino-nucleon scattering,  $\nu N \rightarrow l^\pm N'$ , in the  $(\bar{\nu}_\mu \nu_e)$  and  $(\nu_\mu \bar{\nu}_e)$  runs.

Specific example parameters for the target/detector and for the event sample sizes are given in table 1. Predicted event samples are in the range of millions to tens-of-millions of events and if the experimental uncertainties can be controlled then these sample sizes will correspond<sup>9</sup> to limiting statistical uncertainties of  $\Delta \sin^2 \theta_W = 0.0003$  and  $0.0001$  for the  $(\nu_\mu \bar{\nu}_e)$  and  $(\bar{\nu}_\mu \nu_e)$  beams, respectively, at the 50 GeV nufact and  $\Delta \sin^2 \theta_W = 0.0001$  and  $0.00003$  for the corresponding measurements at 500 GeV. It remains, of course, to be demonstrated that the experimental uncertainties will ever allow these measurement accuracies, but the potential of this measurement is anyway impressive.

#### 4.2 Measurement of the WMA in DIS

The most precise current measurement of  $\sin^2 \theta_W$  from  $\nu$ -N DIS, from NuTeV <sup>19</sup>,

$$\sin^2 \theta_W = 0.2253 \pm 0.0019(\text{stat.}) \pm 0.0010(\text{syst.}) \quad (\text{preliminary}), \quad (30)$$

gives an equivalent uncertainty on the W mass,  $\Delta M_W \simeq 100 \text{ MeV}/c^2$ , that is competitive with direct measurements at colliders. Measurements at nufacts may well extend the historical tradition of neutrino-nucleon DIS experiments in providing some of the most precise measurements of  $\sin^2 \theta_W$ .

The complexity of nucleon targets makes it necessary, as in previous neutrino experiments, to consider NC-to-CC cross section ratios in order to make theoretical sense of the results. Since both the  $(\nu_\mu \bar{\nu}_e)$  and  $(\bar{\nu}_\mu \nu_e)$  beams at nufacts are mixtures of a neutrino and an antineutrino flavor, the appropriate experimental NC-to-CC ratios,  $R_\nu^{\mu-}$  and  $R_\nu^{\mu+}$ , respectively, are each linear combinations of the traditional NC-to-CC cross section ratios for neutrinos,  $R^\nu$ , and antineutrinos,  $R^{\bar{\nu}}$ :

$$R_\nu^{\mu-} \simeq 0.70R^\nu + 0.30R^{\bar{\nu}},$$

$$R_\nu^{\mu+} \simeq 0.63R^\nu + 0.37R^{\bar{\nu}}.$$

Because the linear combinations are so similar, the two measurements will have almost equal numerical values,  $R_\nu^{\mu-} \simeq 0.330$  and  $R_\nu^{\mu+} \simeq 0.332$  for  $\sin^2 \theta_W = 0.225$ , and their physics content will clearly be nearly identical.

Traditional heavy target neutrino detectors could not distinguish  $\nu_e$ -induced CC interactions from NC interactions and this separation will probably be the most demanding experimental requirement for analyses at nufacts. However, with huge statistics and high performance tracking detectors such as those described in section ??, the DIS measurement will presumably eventually be systematically limited by theoretical hadronic uncertainties rather than statistical or experimental uncertainties.

The vastly improved statistics and experimental conditions at nufacts makes it difficult to extrapolate the measurement accuracy from that at today's neutrino experiments. Reference <sup>5</sup> estimates that the predicted uncertainty in  $M_W$  from a nufact analysis might be of order 10 MeV, which improves by an order of magnitude on today's neutrino experiments <sup>19,20</sup> and is approximately equal to the projected best direct measurements from future collider experiments. Thus, the  $\sin^2 \theta_W$  measurement from DIS could be a useful complement to the  $\nu$ -e scattering measurements described in the previous subsection.

## 5 Measurements of CKM Matrix Elements

With huge samples of flavor tagged events, nufacts have the potential to make impressive measurements of the absolute squares of several of the elements in the fundamental Cabbibo-Kobayashi-Maskawa (CKM) mixing matrix that characterises the charged current (CC) weak interactions of quarks. Lower energy nufacts will provide an opportunity for unique and precise measurements of the elements  $|V_{cd}|$  and  $|V_{cs}|$  and further measurements of the more theoretically interesting elements

$|V_{ub}|$  and  $|V_{cb}|$  will become available at the higher energies required for B production. Each of the analyses <sup>9</sup> would involve vertex tagging of heavy final state quarks and will be somewhat analagous to, but vastly superior to, current neutrino measurements of  $|V_{cd}|^2$  that use dimuon events for final state tagging of charm quarks.

Today's measurements of  $|V_{cd}|$  in  $\nu N$  scattering are already the most precise in any process and a fundamental advantage of  $\nu N$  DIS over all other types of CKM measurements is that the scattering process involves the interaction of an external W boson probing the quarks inside a nucleon rather than an internal W interaction inside a hadron. (In principle, the HERA ep collider could also do such measurements, but they turn out not to be feasible in practice.) Such external W probes allow measurements that are theoretically cleaner than other processes because the asymptotic freedom property of QCD predicts quasi-free quarks with reduced influence from their hadronic environment for  $Q$  significantly above the GeV-scale.

Another difference relative to, say, the CKM measurements at B factories is that the measurements are of the magnitudes of individual CKM matrix elements rather than of interference terms. This is understood easily from the naive quark-parton model approximation, where the differential cross sections for quark transitions,  $\frac{d\sigma}{dx}$ , are given as products of quark densities with the absolute squares of matrix elements:

$$\frac{d\sigma}{dx}(d \rightarrow c) \propto x d(x) |V_{cd}|^2 \quad (31)$$

$$\frac{d\sigma}{dx}(s \rightarrow c) \propto x s(x) |V_{cs}|^2 \quad (32)$$

$$\frac{d\sigma}{dx}(u \rightarrow b) \propto x u(x) |V_{ub}|^2 \quad (33)$$

$$\frac{d\sigma}{dx}(c \rightarrow b) \propto x c(x) |V_{cb}|^2, \quad (34)$$

with  $d(x)$ ,  $s(x)$ ,  $u(x)$  and  $c(x)$  the respective initial-state quark densities and these expressions are very approximate only because important threshold correction factors have been neglected.

The  $|V_{cd}|$  analysis at a nufact, with hundreds of millions of vertex-tagged charm events in a high-performance detector, should have profound statistical, experimental and theoretical advantages over today's measurement and may well reach <sup>9</sup> the parts-per-mil level of accuracy. As is evident from equation 32, the measurement of  $|V_{cs}|$  is intrinsically more difficult than  $|V_{cd}|$  because it requires a knowledge of the strangeness content of the nucleon. Reference <sup>9</sup> speculates that  $|V_{cs}|$  could nevertheless be measured at the percent level, which would also become the best direct measurement of the element and would provide a much improved unitarity test on its value.

The B-production analyses at higher energy nufacts should be experimentally rather similar to the charm analyses but would have vastly greater theoretical interest. Both  $|V_{ub}|$  and  $|V_{cb}|$  determine the lengths of sides of the "unitarity triangle" that is predicted to exist if the CKM matrix is indeed unitary. The main goal

of today's B factories is to measure the interior angles of this triangle to confirm that it is indeed a triangle, and the complementary input from a nufact will be an enormous help in this verification process. In particular, the predicted <sup>5,9</sup> 1-2 % accuracy in  $|V_{ub}|^2$  is several times better than predicted accuracies in any future measurements of other processes, and will obviously provide a very strong constraint on the unitarity triangle.

Table 3 summarizes the predicted <sup>9</sup> nufact contributions to determining the CKM matrix elements, giving the current, experimentally determined values for the 9 mixing probabilities along with their current percentage uncertainties and speculative projections <sup>5</sup> for how 4 of the 9 uncertainties might be reduced at a 500 GeV nufact.

Table 3: Absolute squares of the elements in the Cabbibo-Kobayashi-Maskawa (CKM) quark mixing matrix. The second row for each quark gives current percentage uncertainties in the absolute squares and speculative projections of the uncertainties after analyses from a 500 GeV nufact. The measurements of  $|V_{cd}|^2$  and  $|V_{cs}|^2$  might be comparably good for a 50 GeV nufact but  $|V_{ub}|^2$  and  $|V_{cb}|^2$  would not be measured. The uncertainties assume that no unitarity constraints have been used.

	<b>d</b>	<b>s</b>	<b>b</b>
<b>u</b>	<b>0.95</b> ±0.1%	<b>0.05</b> ±1.6%	<b>0.00001</b> ±50% → 1-2%
<b>c</b>	<b>0.05</b> ±15% → 0.2-0.5%	<b>0.95</b> ±35% → ~ 1%	<b>0.002</b> ±15% → 3-5%
<b>t</b>	<b>0.0001</b> ±25%	<b>0.001</b> ±40%	<b>1.0</b> ±30%

## 6 Rare and Exotic Processes

The potential for studying rare and exotic processes at nufacts is limited relative to collider experiments due to the more modest center-of-mass energies. Nevertheless there will still be some opportunities to both further our knowledge of the SM by studying rare processes and to search for processes not predicted by the SM. Examples of a few potential processes involving exotic physics that might be observable at nufacts include:

1. a non-standard flavor-changing neutral current (FCNC) interaction converting valence u quarks to charm quarks,  $u \rightarrow c$ , would appear as an excess of charm events over anti-charm events at high  $x$ . In contrast to FCNC searches in decays, this is a unique opportunity to observe fundamental flavor-changing neutral currents at the quark level <sup>9</sup>
2. some types of unstable exotic neutral leptons <sup>9</sup>
3. R-parity violating SUSY searches <sup>21</sup>



4. hypothetical new neutrino interactions involving microscopic extra dimensions that are much larger than the Planck scale <sup>21</sup>.

## 7 Charm Physics Studies

It should be clear from the discussions in sections 2.3 and 5 that nufact’s will be rather impressive factories for the study of charm – with a clean, well reconstructed sample of several times  $10^8$  charmed hadrons produced in  $10^{10}$  neutrino interactions.

There are several interesting physics motivations for charm studies at a nufact <sup>9</sup>. Measurement of charm decay branching ratios and lifetimes are useful for both QCD studies and for the theoretical calibration of the physics analyses on B hadrons. Charm decays also provide a “clean laboratory” to search for exotic physics contributions since the SM predicts 1) tiny branching ratios for rare decays, 2) small CP asymmetries and 3) slow  $D^0 \rightarrow \bar{D}^0$  oscillations, with only of order 1 in  $10^4$  oscillating before decay.

It is a unique advantage of CC-induced charm production in neutrinos that the production sign of the charm quark is tagged with very high efficiency and purity by the charge of the final state lepton:

$$\begin{aligned} \nu q &\rightarrow l^- c \\ \bar{\nu} \bar{q} &\rightarrow l^+ \bar{c}, \end{aligned} \tag{35}$$

where  $q = d$  or  $s$  and  $\bar{q} = \bar{d}$  or  $\bar{s}$ . This is of particular benefit to oscillation and CP studies, as is the expected precise vertexing reconstruction of the proper lifetime of decays. As an example of the advances in charm studies that might result, particle-antiparticle mixing has yet to be observed in the charm sector and it is quite plausible <sup>5</sup> that a nufact would provide the first observation of  $D^0 - \bar{D}^0$  mixing.

## 8 Summary

It has been shown that nufacts will have unique capabilities for HR neutrino physics, with huge event samples collected in high-performance detectors. The physics reach should extend well beyond traditional neutrino physics topics and should complement or improve upon many analyses in diverse areas of collider and fixed target physics, including:

- the only realistic opportunity, in any physics process, to determine the detailed quark-by-quark structure of the nucleon
- with polarized targets, additionally map out the quark-by-quark spin structure of the nucleon and, perhaps, determine the gluon contribution to the nucleon’s spin
- some of the most precise measurements and tests of perturbative QCD
- some of the most precise tests of the electroweak theory through measurements of  $\sin^2 \theta_W$  with fractional uncertainties approaching the  $10^{-4}$  level

- measurements of the CKM quark mixing matrix that will be interesting for lower energy nufacts ( $|V_{cd}|$  and  $|V_{cs}|$ ) and will become extremely important ( $|V_{ub}|$  and  $|V_{cb}|$ ) at higher energies
- a new realm to search for exotic physics processes
- as a bonus outside neutrino physics, a charm factory with unique capabilities.

The expected experimental conditions at nufacts are so novel and impressive that the topics presented in this paper must surely represent no more than a limited first attempt to understand their full potential for HR neutrino physics.

### Acknowledgments

This work was performed under the auspices of the U.S. Department of Energy under contract no. DE-AC02-98CH10886.

1. An unpublished note by A.C. Melissinos (1960) is the first reference found by K.T. McDonald in a compilation of muon collider accelerator physics prior to 1995 that can be found at <http://www.hep.princeton.edu/mumu/physics/index.html#accel>.
2. The Muon Collider Collaboration,  $\mu^+\mu^-$  Collider: A Feasibility Study, BNL-52503, Fermilab-Conf-96/092, LBNL-38946, July 1996, unpublished.
3. The Muon Collider Collaboration, *Status of Muon Collider Research and Development and Future Plans*, Phys. Rev. ST Accel. Beams, 3 August, 1999.
4. B.J. King, *Assessment of the prospects for muon colliders*, paper submitted in partial fulfillment of requirements for Ph.D., Columbia University, New York (1994), available from LANL preprint archive as *physics/9907026*.
5. B.J. King, *Neutrino Physics at a Muon Collider*, Proc. Workshop on Physics at the First Muon Collider and Front End of a Muon Collider, Fermilab, November 6-9, 1997, *hep-ex/9907033*.
6. S. Geer, *Neutrino Beams from Muon Storage Rings: Characteristics and Physics Potential*, Phys. Rev. **D57**, 6989 (1998).
7. A compilation of papers with physics topics relevant to neutrino factories, compiled by K.T. McDonald, can be found at <http://www.hep.princeton.edu/mumu/nuphys/index.html>.
8. M. Goodman, these proceedings.
9. I. Bigi *et al.*, *The Potential for High Rate Neutrino Physics at Muon Colliders and Other Muon Storage Rings*, contact author B.J. King, to be published.
10. K. Abe *et al.*, *Design and performance of the SLD vertex detector: a 307 Mpixel tracking system.*, NIM A 400 (1997) 287-343.
11. See, for example, Chris Quigg, *Neutrino Interaction Cross Sections*, FERMILAB-Conf-97/158-T.
12. NuFact'99, Lyon, 5-9 July, 1999, <http://lyoinfo.in2p3.fr/nufact99/general.html>.
13. A. Petrov, these proceedings.
14. D. Babusci *et al.*, Proc. 11th Int. Symp. High-Energy Spin Phys., AIP Conf. Proc. 343, p.523 (1995).

15. D.G. Crabb and W. Meyer, *Solid Polarized Targets for Nuclear and Particle Physics Experiments*, Ann. Rev. Nucl. Part. Sci. 1997, 47:67-109.
16. See, for example, A. Deshpande, *The Physics Case for Polarized Protons at HERA*, hep-ex/9908051.
17. J. Ashman *et al.*, the EMC Collaboration, Phys. Lett. B **206** (1988) 364.
18. Private communication with P. Rehak.
19. K.S.McFarland, NuTeV collaboration, to be published in the proceedings of the XXXIIIrd Rencontres de Moriond (1998).
20. C.Arroyo *et. al.*, Phys. Rev. Lett. **72**, 3452 (1994).
21. Private communication with F. deJongh.